ONLINE SUPPLEMENTARY INFORMATION

Supplementary Methods

Lung Function Measurement and Analysis

Lung function measurements were obtained by FlexiVent plythesmography (Scireq, Montreal) as we previously described.[2] Lung function measurements were obtained by FlexiVent plythesmography (Scireq, Montreal). Mice were sedated with Euthasol followed by a tracheostomy with an 18G, 12 mm blunt stainless steel needle (LS18, Instech Laboratories). Mechanical ventilation was performed at the rate of 150breaths/min and positive end-expiratory pressure of $3cmH_20$. The FlexiVent software recorded all Force Pulmonary Maneuvers. Following pulmonary function measurements, mice were exsanguinated and lungs were were removed en bloc. Tissue was processed for AEC2 or collagen isolation or was fixed in 10% formalin for histology.

Lung Histology, Mean Linear Intercept Analysis and TUNEL in situ

Isolated lungs were instilled with PBS at constant fluid pressure of $30cmH_20$ for 3minutes, then submerged in 10% formalin (Richard-Allen Scientific 531201) overnight at 4ºC for at least 12hours for fixation. Processing of fixed tissue for histology was performed as previously described.[2] Briefly, three changes of PBS and one change into 70% ethanol preceded storage in 100% ethanol at -20ºC. Dehydration in graded changes of ethanol and then into xylene preceded paraffin embedding. Both transverse and frontal 5 µm sections were cut, placed on supercharged glass slides and deparaffinized with xylene and an ascending ethanol series. Sections were stained with hematoxylin & eosin (H&E) or Hart's reagent according to standard methods.

M*ean linear intercept (MLI)* was determined as previously described[3] from images obtained by light microscopy of H&E stained sections at 40X magnification. Both transverse and frontal sections were

examined. Sixteen randomly selected regions of lung parenchyma per sample (4 images per section) were evaluated by overlaying a reference grid. MLI was calculated by dividing total grid length by the number of alveolar wall to grid line intersections per section. For each experimental cohort, the median MLI for all histological images/individual sample was calculated and graphed.

Lung parenchymal cell DNA damage was detected by the Click-iT® TUNEL Assay kit (Molecular Probes, Life Technologies) used according the manufacturer's protocol. Formalin fixed 5µm sections were deparaffinized, treated with proteinase K and then with Click-iTEdUTP and TdT enzyme at 37ºC. Nuclei were labeled with DAPI. A positive control was generated by DNAse1 treatment. TUNEL positive cells were identified manually in 40X images. The percent of TUNEL positive alveolar epithelial cells divided by the total number of DAPI stained nuclei per image per animal was determined for each cohort.

SPC Staining and cell counts

Lungs tissue sections were stained with SP-C antibody to quantitate the total number of AEC2. Briefly, 5µm lung tissue sections were deparaffinized and rehydrated in xylene, heated in 10 mM citrate buffer (pH 6.0), blocked with 2% normal goat serum, and incubated with primary antibody rabbit anti-proSP-C (1:200, Seven Hills) at 4°C for overnight followed by incubation with secondary conjugated antibody goat anti-rabbit Cy3 (1:250, Jackson ImmunoResearch Laboratories) for 1 hour at room temperature. The nuclei were stained with DAPI. Images were taken with Leica Fluorescence Upright microscope. The numbers of cells positive for SPC were obtained by counting total 20 fields at 20X magnification. FIJI imaging software (Image J, NIH) was used for SPC quantitation. Images were color thresholded to define the intensity values for the SPC signal only. Each signal was quantified and the percent was determined from the total number of nuclei per image.

Collagen and Elastin Quantitation

Total lung collagen content was estimated as hydroxyproline. Briefly, lungs were dissected and heart, thymus, and large airways were removed. Lungs were gently dried, weighed, and homogenized in water (100ul per 10 mg of lung), then analyzed using the Total Collagen kit from BioVision (K218-100). The amount of hydroxyproline was determined against a standard curve generated using known concentrations of hydroxyproline (Sigma).

Lung sections were stained for elastin by Hart's reagent (resorcin-fuchsin solution) overnight at room temperature. Slides were counterstained in 0.5% tartrazine in 0.25% acetic acid. Images were collected using a Leica DMI6000B microscope with a Leica DRC295 camera at 0X magnification. Images of 3 transverse sections/sample were collected and imaged (16 images/slide). FIJI imaging software (Image J, NIH) was used for elastin quantitation. Images were color thresholded to define the intensity values for the elastin. This value was normalized to a duplicate image that was binarized to quantify the area of total lung tissue. Percent elastin was calculated by dividing the number of pixels corresponding to elastin stained black by total lung tissue stained yellow and black. For each experimental cohort, the median percent elastin in all histological images/individual sample was calculated and graphed.

Mitochondrial Bioenergetics

AEC2 were isolated from mouse whole lung.[4]. Cells were seeded at 40,000 per well onto a 96-well plate (Seahorse Biosciences) coated with 5ug/cm2 of Cultrex Mouse Laminin 1 (Trevigen). Growth conditions to maintain AEC2 in culture were in complete media (DMEM supplemented with 5ug/ml Insulin, 5ug/ml transferrin, 5ng/ml sodium selenite, 1mM L-glutamine, 0.25% bovine serum albumin, 10mM Hepes, 0.1mM non-essential amino acids, 10% fetal bovine serum, 1X penicillum-streptomycin-amphotericin B).[5] After 60hours, medium was changed to basal media (Seahorse Biosciences) supplemented with 4mM L-glutamine, 25mM D-glucose, and 2mM Pyruvate. The XF96 Extracellular Flux Analyzer (Seahorse Biosciences) was used to measure oxygen consumption rate (OCR). Initial optimization was performed using a series of titration experiments to determine the concentration that

elicited maximal responses. The effects of mitochondrial inhibitors on OCR were assessed approximately 1h after incubation at 37ºC without CO2, followed by basal oxygen consumption measurements. XF96 Extracellular Flux Analyzer raw data output was transformed to Seahorse WAVE software to obtain a cellular bioenergetics profile for each cohort.

Western Blotting and Antibodies

Western blotting was performed as previously described[2]. Briefly, isolated cell pellets were lysed on ice for 30 minutes in RIPA buffer containing a protease inhibitor cocktail. Lysates were clarified by centrifugation at 14K rpm for 15minutes at 4C. Soluble cellular proteins were resolved by SDS-PAGE, transferred onto polyvinylidenedifluoride (PVDF) membranes, and blocked with 5% nonfat milk in TBST buffer for 1 hour at room temperature. Antibodies used were phospho-Akt (Thr308; Cell Signaling, 9275), phospho-MDM2 (Ser166; Cell Signaling, 3521), phospho-PTEN (Ser380, Thr382,/383; Cell Signaling, 9549), phospho-p53 (Ser15; Cell Signaling, 9284), BAX (Santa Cruz Biotechnology, sc-7480), SIRT1 (Sigma, HPA006295), PGC1alpha (ABCAM, ab54484), and Beta-actin (Cell Signaling, 4967), and horseradish peroxidase-labeled secondary antibodies. Blots were treated with Pico ECL Plus and visualized on Fujifilm. Densitometry data was obtained using ImageJ.

Supplemental Results

Impact of Resveratrol treatments on lung ECM

Collagen content was assessed by measuring total hydroxyproline in whole lung one month after the last Resveratrol treatment. As previously reported by others,[6] collagen content in WT controls rose in aged mice, though this change was not significant between 2 and 5 months of age. This was also true for collagen content of 2 and 5 month-old terc-/-F2 mice, which showed no significant difference from WT age-matched samples. Thus, at the younger ages at which prophylactic Resveratrol treatments were administered, no significant changes in hydroxyproline content of the whole lung were observed in

untreated mice, and, unsurprisingly, Resveratrol treatment had no notable impact over this age span (Supplemental Figure 1A).

Elastin quantitation was performed using ImageJ quantitation of photomicrographs of transverse lung sections in which alveolar wall elastin was stained using Hart's stain.[7] Samples from Resveratrol and PBS treated and untreated terc-/-F2 cohorts, as well as tissue from young and old WT mice, were analyzed. This analysis demonstrated no significant changes in alveolar elastin content in Resveratrol-treated 5 month-old terc-/-F2 mice when compared to tissue from untreated terc-/-F2 mice (Supplemental Figure 1B). Thus, while we did not observe substantial changes in ECM modification in Resveratrol-treated mice, we also noted that the ECM compartment was not adversely affected at this early stage of lung aging in terc-/-F2 lung. These data indicated that at 5 months of age, other lung components were responsible for the altered pulmonary function observed in untreated animals, which also served as targets for Resveratrol treatments.

Impact of Resveratrol treatments on AEC2 mitochondrial bioenergetics

We next investigated AEC2 mitochondrial bioenergetics using the Seahorse Assay, which measures oxygen consumption rate (OCR) *in vitro*. We first determined changes in the bioenergetics of isolated AEC2 from young (2-5 months old) and middle- to old-aged (9-16 months old) terc-/-F2 mice (Supplemental Figure 2A). Mitochondria in aged terc-/-F2 mice had a significant decline in OCR compared to both younger terc-/-F2 and WT mice. These data indicated that changes in mitochondria were significantly exacerbated with age and that AEC2 mitochondria become less efficient during lung aging in terc-/-F2. We then analyzed the effect of Resveratrol treatments in vivo on the OCR, as measured one-month after the last treatment. This analysis showed no significant improvement in mitochondrial OCR in AEC2 isolated from 5 month-old Resveratrol-treated mice compared to OCR in AEC2 from 5 month-old vehicle-administered and untreated controls (Supplemental Figure 2B). Thus, despite maintenance of PGC-1alpha expression in AEC2 isolated from Resveratrol treated lungs

(Figure 5), the impact of Resveratrol treatments on mitochondrial function at this early stage of lung aging was negligible. We speculate that these contradictory findings may be due to a lag in impact on mitochondrial bioenergetics from decreasing levels of PGC-1alpha in 5 month-old terc-/-F2 mice and that this impact does not become significant until animals are considerably older than 12 months, well past the point of cessation of Resveratrol treatment analysis in our study.

Supplemental Figures and Legends

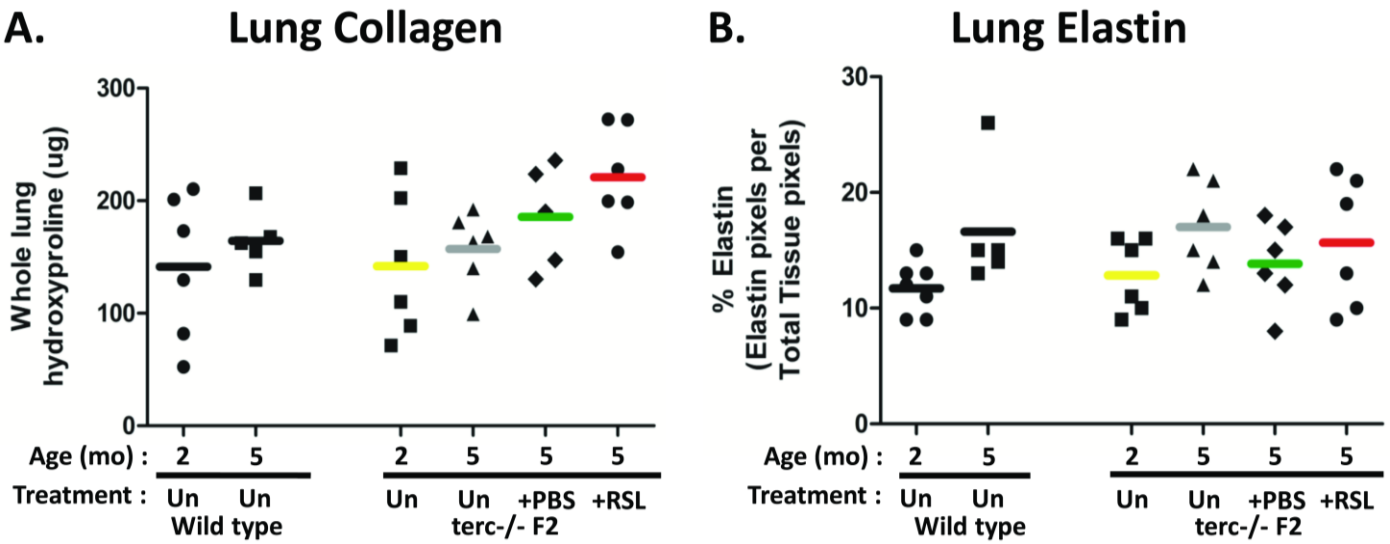

Supplemental Figure 1. Lung collagen and elastin content following Resveratrol treatment. A) Total whole lung hydroxyproline levels. Each data point represents a single animal, with the value calculated as an average of triplicate measurements and bar represents the mean per group. Hydroxyproline content was analyzed on lungs between all groups (N=5-6 in each group) with no statistical significance. **B)** Elastin quantitation in F2 terc null mice by image analysis. Hart's staining for elastin was performed on 5 micron paraffin lung sections for all mice. Data are expressed as percent elastin (black) pixels measured per total tissue (black and yellow). For each mouse 15 images were analyzed with 3 mice in each group. The elastin content over these groups was not significantly

different. Statistical analysis was performed by using 1-way Analysis of Variance Bonferroni multiple comparison test.

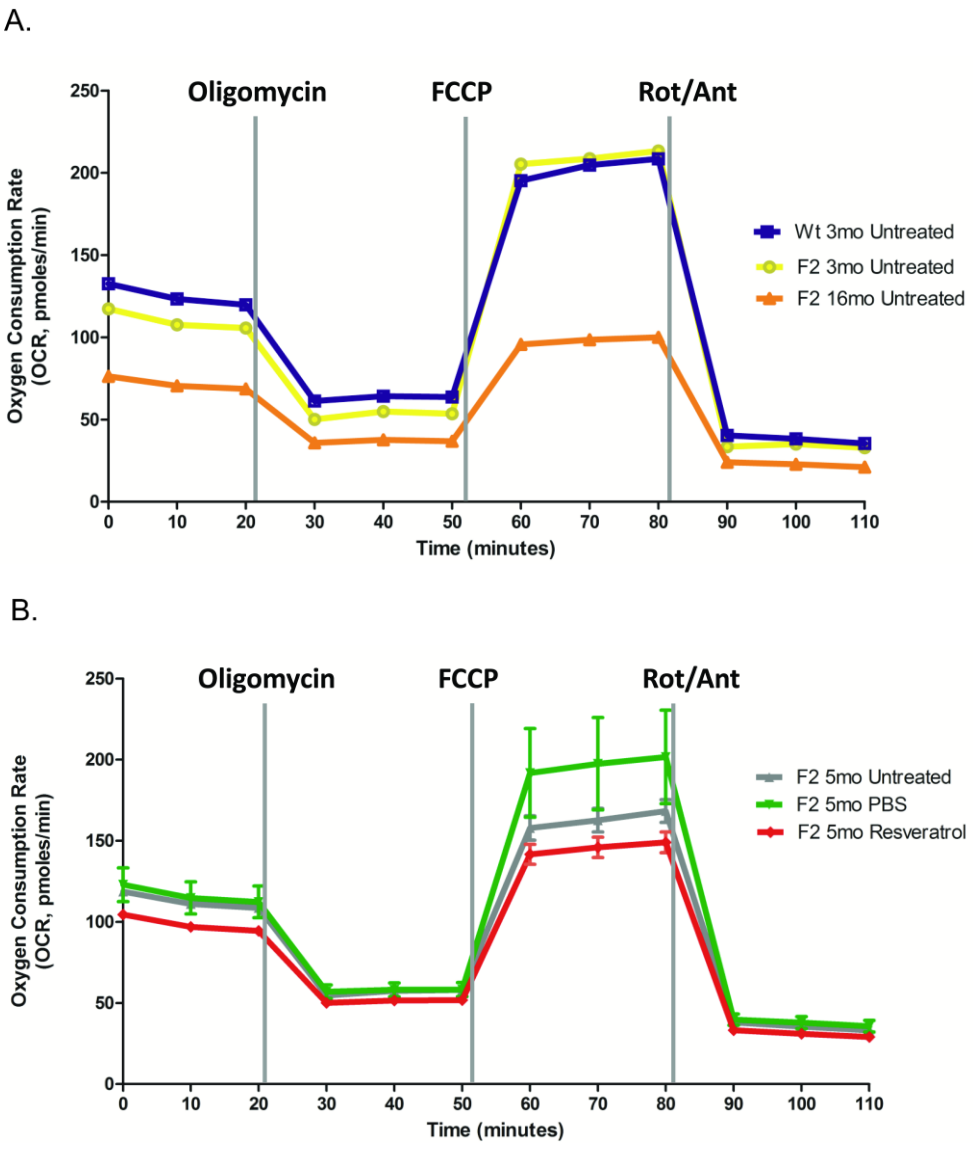

Supplemental Figure 2. Mitochondrial function in cultured AEC2 at baseline and following Resveratrol treatment. A) Aged AEC2 from 16 month-old terc-/-F2 mice had an overall lower mitochondrial OCR profile compared to the profile derived from AEC2 isolated from 3 month-old terc-/-F2 and WT mice. The baseline OCR was first measured followed by subsequent and sequential addition of oligomycin (1 µM), FCCP (0.5µM) and rotenone (0.5 µM) plus antimycin A (0.5 µM). Oligomycin, an ATP synthase complex inhibitor, reduces OCR, while addition of ATP synthesis

uncoupler FCCP restores OCR and was used to measure the capacity of mitochondria to respond to this stimulus. Addition of rotenone (complex I inhibitor) and antimycin A (complex III inhibitor) completely blocks OCR. The changes in OCR are expressed (pmoles/min) and the values are mean of biological replicates from N= 2 mice per group. **B)** OCR was measured in AEC2 from terc-/-F2 lung 1 month after the last Resveratrol treatment. The OCR profile measured in isolated and cultured AEC2 was unchanged when all three groups (AEC2 isolated from 5 month-old terc-/-F2 either Resveratrol-treated, vehicle-administered or untreated) were compared The changes in OCR are expressed (pmoles/min) and the values are mean ± SEM of N=4 mice per group, analyzed in triplicate.

REFERENCES

1. Gertz M, Fischer F, Nguyen GTT, et al. Ex-527 inhibits Sirtuins by exploiting their unique NAD(+)-dependent deacetylation mechanism. P Natl Acad Sci USA 2013;**110**(30):E2772-E81.

2. Garcia O, Hiatt MJ, Lundin A, et al. Targeted Type 2 Alveolar Cell Depletion. A Dynamic Functional Model for Lung Injury Repair. Am J Respir Cell Mol Biol 2016;**54**(3):319-30.

3. Lee J, Reddy R, Barsky L, et al. Lung alveolar integrity is compromised by telomere shortening in telomerase-null mice. Am J Physiol Lung Cell Mol Physiol 2009;**296**(1):L57-70.

4. Lee J, Reddy R, Barsky L, et al. Contribution of proliferation and DNA damage repair to alveolar epithelial type 2 cell recovery from hyperoxia. Am J Physiol Lung Cell Mol Physiol 2006;**290**(4):L685-L94.

5. Demaio L, Tseng W, Balverde Z, et al. Characterization of mouse alveoalr epithelial monolayers. Am J Physiol Lung Cell Mol Physiol 2009;**296**(6):L1051-8.

6. Huang K, Mitzner W, Rabold R, et al. Variation in senescent-dependent lung changes in inbred mouse strains. J Appl Physiol (1985) 2007;**102**(4):1632-9.

7. Srisuma S, Bhattacharya S, Simon DM, et al. Fibroblast growth factor receptors control epithelial-mesenchymal interactions necessary for alveolar elastogenesis. Am J Respir Crit Care Med 2010;**181**(8):838-50.